Electrochemically Partitioned Assembly of Organosulfur Monolayers and Nanoparticles

ARTICLE *in* THE JOURNAL OF PHYSICAL CHEMISTRY B · NOVEMBER 2006

Impact Factor: 3.3 · DOI: 10.1021/jp063100l · Source: PubMed

Electrochemically Partitioned Assembly of Organosulfur Monolayers and Nanoparticles

Peng Diao,*,† Min Guo,‡ Qunchao Hou,† Min Xiang,† and Qi Zhang†

Department of Applied Chemistry, School of Materials Science and Engineering, Beijing University of Aeronautics and Astronautics, Beijing 100083, People's Republic of China, and Department of Physical Chemistry, University of Science and Technology Beijing, Beijing 100083, People's Republic of China

Received: May 20, 2006; In Final Form: July 31, 2006

Partitionally assembled organosulfur monolayers were prepared by using an electrochemically assisted assembly method on gold films that were preseparated into two regions insulated from each other. Cyclic voltammetry (CV) and X-ray photoelectron spectroscopy (XPS) were employed to characterize the *n*-dodecanethiol (DDT) and the 11-mercaptoundecanoic acid (MUA) monolayers, which were separately assembled on different substrate regions. CV results indicated that both the DDT- and MUA-coated gold electrodes showed a blocking property toward the negatively charged redox probe $Fe(CN)_6^{3-}$. However, when positively charged $Ru(NH_3)_6^{3+}$ was used as the redox probe, the MUA- and DDT-modified electrodes showed quasireversible and blocking CV features, respectively. These phenomena were attributed to different interactions between the negatively charged MUA surface and the negatively or positively charged redox probes. XPS spectra obtained on the MUA modified region exhibited an O(1s) peak and a small discrete C(1s) peak, which arose from the oxygen and the carbon atoms in the carboxylic acid groups, respectively. For the DDT-modified region, these two peaks were absent. CV and XPS experimental results provided strong evidence that different SAMs were selectively deposited onto different regions of the preexisting patterns of the substrate by electrochemically partitioned assembly. The partitionally assembled sulfur-based monolayers with different terminal groups were used to form location-selective nanoparticle assemblies. This electrochemically partitioned assembly technique has great potential in controllable constructions of molecular layers and nanostructures on different surface microarchitectures that are closely integrated on one substrate but insulated from each other.

1. Introduction

The sulfur-based self-assembled monolayers (SAMs) formed on gold have been of great interest for more than 2 decades,[1] because they find applications in many fields such as interfacial charge-transfer studies,[2] wetting control,[3] molecular recognition,[4] and fabrication of nanoparticle assemblies.[5] Ease of preparation is one of the most attracting features of sulfur-based SAMs. However, the simplicity of SAM preparation offers little flexibility in controlling the formation of SAMs. Since the ability of preparing SAMs with different functional groups in different substrate regions is very important to many applications, the formation of location-selective assemblies is one of the key issues that chemists in this field aim to solve. Although great success has been achieved in forming mesoscale SAM patterns by the "microcontact printing" technique,[6] with which one can limit the formation of SAMs within the regions that have contact with "the stamp" predipped with organosulfur molecules, it is still challenging to prepare SAM patterns whose size, shape, and location are determined by the features of artificial structures prefabricated on the substrates.

Applying potentials to the substrates during assembly is another way to control the formation of SAMs.[7] It has been demonstrated that highly negative potentials lead to the reductive desorption of organosulfur SAMs,[7a−c] whereas positive potentials accelerate the assembly process.[7e,f] Although electrochemical methods are proved to be good approaches to the controllable formation of SAMs, only a few works have been reported to prepare location-selective SAMs using electrochemical methods.[8,9] Coadsorption of *n*-alkanethiols and functionalized alkanethiols with a marked difference either in chain length or in molecular structure can lead to the formation of phase-separated binary SAMs,[10] and each SAM phase has a different desorption potential.[8,10e−g] This makes it possible to selectively desorb one component in the binary SAMs by electrochemical means and then to site-selectively readsorb another organosulfur molecules at the locations where the desorbed component is initially occupied.[8] Obviously, in this method, the readsorption locations are determined by different component domains randomly formed in the original phase-separated binary SAMs. By electrochemical oxidation of alkyl thiosulfates in a tetrahydrofuran solution, Freund et al. have successfully prepared SAMs on one set of the two closely spaced gold microelectrode arrays, while leaving the other set unmodified.[9a] They have not shown, however, whether their method is suitable for the fabrication of so-called "partitionally assembled monolayers", that is, different monolayers are separately assembled on different substrate regions. Lopez and co-workers have showed that, by combining the self-assembly and the electrochemical desorption techniques, two SAMs can be separately deposited on two surface regions which were generated from one substrate by laser ablation.[9b] To minimize the cross-contamination induced by displacement of preformed monolayer constituents by molecules of another alkanethiol during the self-assembly for the second monolayer,

* Corresponding author. Tel & Fax: 86-10-8231-6841. E-mail: pdiao@buaa.edu.cn.
† Beijing University of Aeronautics and Astronautics.
‡ University of Science and Technology Beijing.

10.1021/jp063100l CCC: $33.50
Published on Web 09/07/2006

Lopez et al. reduced the assembly time to 1 min, which according to the kinetic studies by atomic force microscopic,[11a] contact angle,[11b] and electrochemical[11c] measurements is too short to form densely packed, well-ordered, and pinhole-free SAMs. Applying positive potentials to the substrate region where the second SAMs are expected to form might be a feasible solution to this issue, since it has been demonstrated that positive potentials significantly quicken the assembly of monolayers.[7e,f] However, to the best of our knowledge, no such work has been reported.

The SAMs terminated with functional groups can be employed as linking layers to construct surface-bound nanostructures using nanoscaled materials as building blocks.[5,6d−f,12,13] Since many applications of nanodevices require well-organized nanostructures, controlled formation of nanostructures from nanoparticles arouses great interests. Selective assembly of nanoparticles on a solid surface is an important aspect in this area and has achieved great progress by atomic force microscopy (AFM) assisted nanolithography[14] and microcontact printing.[6d−f,12] However, AFM-assisted nanolithography is inconvenient to prepare large-area (several square micrometers or larger) nanoparticle assemblies due to the limitations of AFM tips. On the other hand, the microcontact printing technique can conveniently produce large-area region-selective nanoparticle assemblies, but the sizes and shapes of the assembled regions are determined by the stamp, not the features prefabricated on the substrates.

Herein, we report the selective formation of different SAMs on different substrate locations by an electrochemically partitioned assembly method, which combines the self-assembly, the electrochemically directed desorption, and the potential-assisted adsorption techniques. We also demonstrate its application in fabricating location-selective nanoparticle assemblies.

2. Experimental Section

Chemicals. The *n*-dodecanethiol (DDT, $HS(CH_2)_{11}CH_3$), 11-mercaptoundecanoic acid (MUA, $HS(CH_2)_{10}COOH$), and the *p*-aminothiophenol (*p*-ATP) were purchased from Aldrich Co and used without further purification. $LiClO_4$ was purchased from Aldrich Co. $Ru(NH_3)_6Cl_3$ and $K_3Fe(CN)_6$ were purchased from Alfa Aesar (A Johnson Matthey Co.) and Beijing Chemical Reagents Co., respectively. All chemicals used in this work were of analytical grade. The DDT, MUA, and *p*-ATP solutions were prepared by dissolving DDT, MUA, and *p*-ATP in absolute ethanol, respectively, and the final concentration for each of them was 1 mM. $LiClO_4$ (0.1 M) was used as the supporting electrolyte.

Electrochemically Partitioned Assembly of Monolayers. Gold substrates were prepared on Si wafers by sputtering with 150 nm Au (99.99%). A 10-nm Cr layer was deposited prior to Au deposition to improve adhesion to the Si wafer. A 5 μm wide insulating gap was used to separate the gold films into two isolated regions. Prior to use, the gold substrates were cleaned in the piranha solution (1:3, 30% H_2O_2:concentrated H_2SO_4, volume ratio) at 90 °C for 5 min followed by rinsing with copious water and absolute ethanol, successively. The strategy for the electrochemically partitioned assembly is schematically shown in Scheme 1. The substrate prefabricated with two closely spaced gold electrodes (M and N electrodes), which were insulated from each other, was first immersed in a 1 mM DDT solution for 12 h to form DDT SAMs on both electrodes (step 1 in Scheme 1). Then, in the second step, the substrate was immersed in a 1 mM MUA ethanolic solution with 0.1 M $LiClO_4$ as the supporting electrolyte. Under intense agitation, a desorption potential (−1.5 V vs SCE) was applied to the M electrode to remove the DDT SAM formed in the first step (step 2 in Scheme 1). After electrochemical desorption for 5 min, which was quite enough for the desorbed DDT molecules to diffuse from the electrode surface to the bulk MUA solution, an adsorption potential (0.4 V vs SCE) was applied to the M electrode for 5 min to form a MUA monolayer (see step 3 in Scheme 1). Alternatively, for the electrochemically directed formation of the *p*-ATP monolayer, a lower adsorption potential of 0.1 V was applied to the substrate because the *p*-ATP SAM begins to be oxidized at about 0.4 V.[15]

SCHEME 1: Schematic Representation of Electrochemically Partitioned Assembly

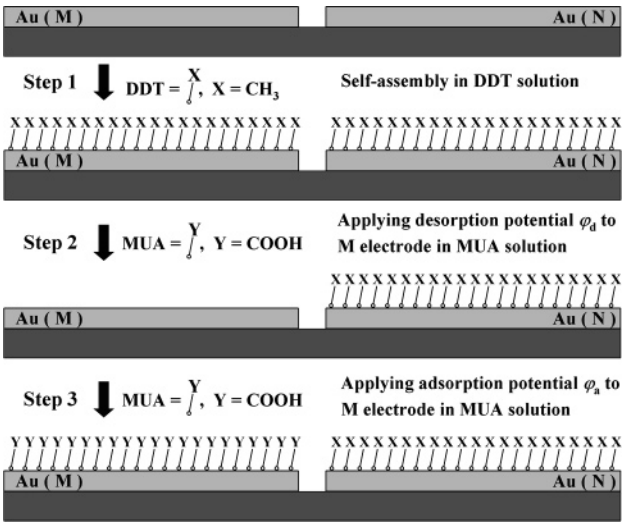

Location-Selective Adsorption of Gold Nanoparticles. Gold colloids were prepared by the Frens method,[16] and the average diameter of colloidal nanoparticles was about 13 nm. Before use, the pH of the colloid solution was adjusted to 4.5. The above-mentioned gold substrates with two separate regions modified with DDT and *p*-ATP SAMs, respectively, were immersed in the gold colloid for 6 h to form a nanoparticle assembly on the *p*-ATP SAM-coated region. After the immersion, the substrates were briefly exposed to ultrasonic cleaning in water to get rid of the gold nanoparticles physically adsorbed on the DDT monolayers and then rinsed with copious water.

Electrochemical Measurements. Cyclic voltammetric measurements were performed on a CHI660A electrochemical workstation (CH Instruments Co.). All CV experiments were carried out in a conventional three-electrode cell at room temperature. A saturated calomel electrode (SCE) and a Pt foil were employed as reference and counter electrodes, respectively. All potentials are reported with respect to SCE.

X-ray Photoelectron Spectroscopic (XPS) Characterization. The samples used in XPS measurements were prepared on relatively large gold substrates, which were also separated into two isolated regions by a 5 μm wide gap. The selective formation of different SAMs on different gold surface regions followed the strategy described above. After formation of SAMs, the whole substrate was put into the chamber of the XPS instrument and the XPS spectra were recorded on each gold surface region. The XPS measurements were carried out on an AXIS-Ultra instrument from Kratos Analytical using monochromatic Al Kα radiation (225 W, 15 mA, 15 kV) and low-energy electron flooding for charge compensation. To compensate for the surface charge effects, all binding energies were calibrated using the C(1s) hydrocarbon peak at 284.80 eV.

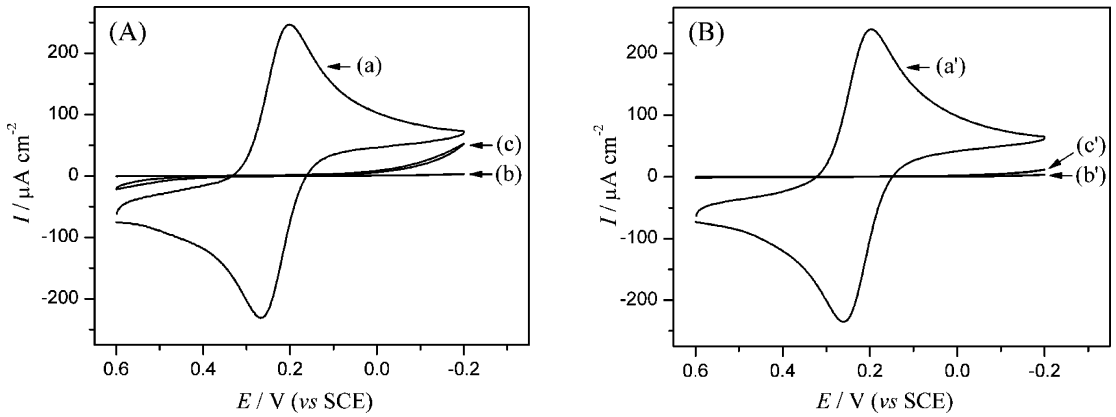

Figure 1. Cyclic voltammograms of M (A) and N (B) electrodes in 1 mM $K_3Fe(CN)_6$ solution after different modification steps shown in Scheme 1: (a, a′) bare gold electrodes, (b, b′) after step 1, (c, c′) after step 3. Supporting electrolyte, 1 M KCl; scan rate, 0.1 V·s^{-1}.

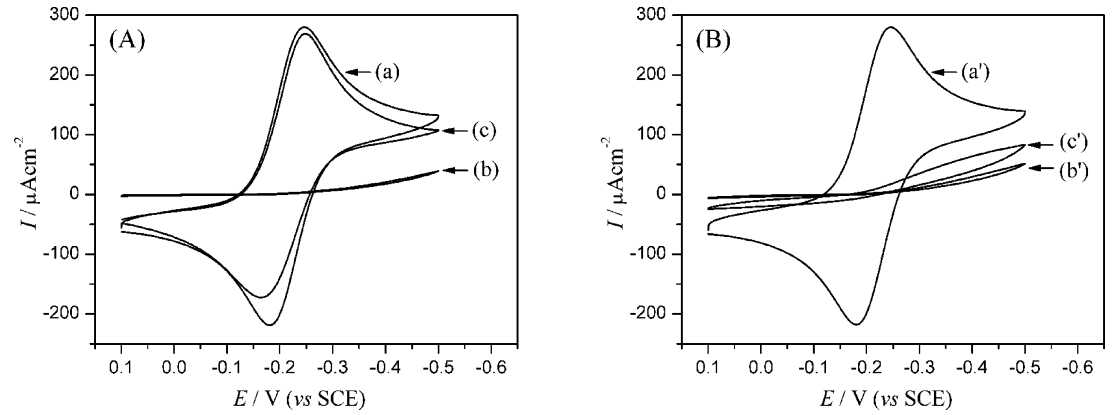

Figure 2. Cyclic voltammograms of M (A) and N (B) electrodes in 1 mM $Ru(NH_3)_6Cl_3$ solution after different modification steps shown in Scheme 1: (a, a′) bare gold electrodes, (b, b′) after step 1, (c, c′) after step 3. Supporting electrolyte, 1 M KCl; scan rate, 0.1 V·s^{-1}.

Scanning Electron Microscopic (SEM) Characterization. The micrographs of assembled nanoparticle monolayers were obtained on a Philips FEI XL30 SFEG scanning electron microscope with an accelerating potential of 10 kV.

3. Results and Discussion

Characterization of Organosulfur Monolayers Prepared by Electrochemically Partitioned Assembly. The MUA monolayer is negatively charged due to the disassociation of terminal COOH groups in a neutral solution, and it repels the anions and attracts the cations. As a result, the MUA monolayer blocks the electron transfer between the negatively charged electroactive species and the underlying gold electrode, while it allows the access of positively charged electroactive species to the gold surface where electron transfer can occur.[17] Accordingly, the strategy of preparing partitionally assembled monolayers on two closely spaced electrodes can be tested by using electroactive species with opposite charges, such as $Fe(CN)_6^{3-}$ and $Ru(NH_3)_6^{3+}$.

Figure 1 shows the cyclic voltammograms of the M and N electrodes in the $Fe(CN)_6^{3-}$ solution after the different modification steps represented in Scheme 1. For both electrodes, the reversible redox peaks at bare electrodes disappear after self-assembly for 12 h in the DDT solution (curves b and b′ in Figure 1), indicating that the DDT monolayers are formed on both electrodes and that they greatly retard the heterogeneous electron transfer between $Fe(CN)_6^{3-}$ and the gold electrodes.[18] After reductive desorption of the DDT SAM (step 2 in Scheme 1), a reversible CV curve returns at the M electrode in the $Fe(CN)_6^{3-}$ solution (data not shown), suggesting removal of the DDT monolayer from the M electrode. While the CV feature at the N electrode (data not shown) remains almost the same as that of curve b′, implying that the electrochemically directed desorption process on the M electrode has no effect on the integrity of the DDT monolayer formed on the nearby N electrode in the first modification step.

After electrochemically directed formation of the MUA monolayer on the M electrode (step 3 in Scheme 1), both M and N electrodes give similar sigmoidal CV responses (curves c and c′ in Figure 1), which are characteristic of blocked electrodes. As mentioned above, the reblocking of the M electrode is due to the repelling effect between the negatively charged $Fe(CN)_6^{3-}$ ions and the terminal COO^- groups of the MUA monolayer. The unchangeable blocking property of the N electrode (curve c′ in Figure 1B) is attributed to the well-kept integrity of the DDT monolayer during the electrochemically directed adsorption process on the nearby M electrode. We believe that, during the overall potential-induced desorption and adsorption processes, the DDT monolayer formed in the first step on the N electrode remained almost intact because of the following two reasons: (1) no desorption potential was applied to the N electrode to remove the DDT monolayer, and (2) the MUA molecules cannot replace the well-assembled DDT molecules from the DDT monolayer within such a short duration of steps 2 and 3 (about 15 min),[19] though the N electrode was also immersed in the MUA solution.

Parts A and B of Figure 2 show the CV responses for M and N electrodes, respectively, after the different modification steps represented in Scheme 1, with 1 mM $Ru(NH_3)_6^{3+}$ as the redox probes and 1 M KCl as the supporting electrolyte. It is seen

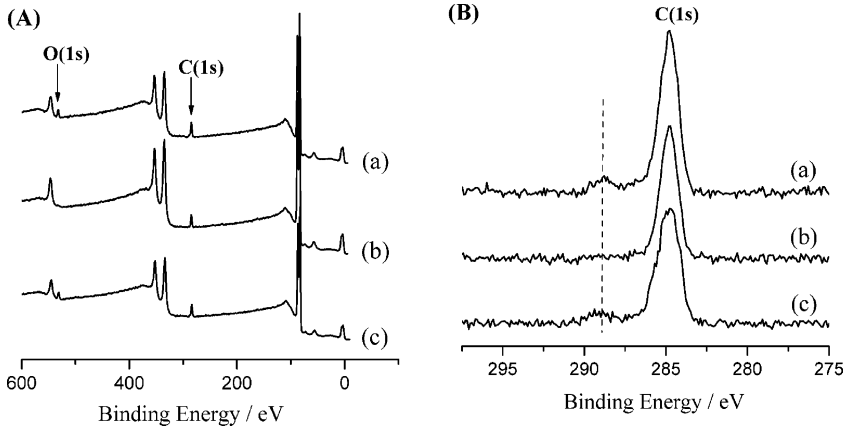

Figure 3. XPS of organosulfur monolayers on gold: survey spectra (A) and high-resolution spectra of the carbon 1s region (B). The spectra were obtained at (a) M electrode after step 3 in Scheme 1, (b) N electrode after step 3 in Scheme 1, and (c) gold substrate after being immersed in 1 mM ethanol solution of MUA for 12 h.

clearly from curves b and b′ of Figure 2 that, when the self-assembly of the DDT monolayer is finished (step 1 in Scheme 1), both the M and N electrodes show sigmoidal CV curves though $Ru(NH_3)_6^{3+}$ is an electrochemically reversible, one-electron, outer-sphere redox couple,[20a,b] indicating that both electrodes are coated with the DDT SAM. By comparing curves a, a′, b, and b′ in Figure 2 with the corresponding ones in Figure 1, two features are immediately apparent: (1) the CV responses for both $Ru(NH_3)_6^{3+}$ and $Fe(CN)_6^{3-}$ at the DDT-monolayer-coated gold electrodes are similarly blocking, and (2) the redox currents for $Ru(NH_3)_6^{3+}$ are larger than those for $Fe(CN)_6^{3-}$ at bare and film-coated electrodes, as expected from the larger heterogeneous rate constant for the redox reaction of $Ru(NH_3)_6^{3+/2+}$ couple compared to that for $Fe(CN)_6^{3-/4-}$ couple.[20] The similar CV responses for both $Ru(NH_3)_6^{3+}$ and $Fe(CN)_6^{3-}$ at the DDT-modified electrodes demonstrate the generality of the blocking behaviors of the DDT SAM for both the positively charged and the negatively charged redox couples, which is in good agreement with previous reports.[17b,18a]

When potential-assisted adsorption of the MUA monolayer on the M electrode was completed (step 3 in Scheme 1), the M electrode gives quasireversible CV response in $Ru(NH_3)_6^{3+}$ solution (curve c in Figure 2A), which is dramatically different from the blocking feature obtained in $Fe(CN)_6^{3-}$ solution (curve c of Figure 1A). This phenomenon is attributed to the attracting effect between the negatively charged COO^- groups and the positively charged $Ru(NH_3)_6^{3+}$ ions, which allows the penetration of $Ru(NH_3)_6^{3+}$ through the MUA monolayer to the gold surface. For the N electrode, as mentioned above, the DDT SAM remained almost intact during electrochemically directed desorption of the DDT monolayer and subsequent adsorption of the MUA monolayer on the nearby M electrode. As a result, the N electrode still exhibits blocking due to the retarding effect of the DDT monolayer to either negatively or positively charged redox probes. Then, after modification step 3, the different CV features for the M electrode in $Ru(NH_3)_6^{3+}$ and $Fe(CN)_6^{3-}$ solutions and the similar CV features for the N electrode in the above-mentioned two solutions provide solid evidence that different SAMs are formed on two closely spaced gold electrodes. This unusual SAM terminal group dependence of the CV behavior at two different electrodes that are integrated on one substrate may find potential applications in developing electrochemical multidetection devices.

A MUA molecule contains 11 carbon atoms with different valence states and two oxygen atoms, while a DDT molecule contains 12 carbon atoms with the same valence state and no oxygen atom. So XPS can provide further evidence for the electrochemically partitioned assembly represented in Scheme 1. The results are shown in Figure 3. After the modification step 3, the XPS spectrum of the M electrode (spectrum a in Figure 3A) resembles that of the gold electrode immersed in the MUA solution for 12 h (spectrum c in Figure 3A). In detail, the characteristic O(1s) peak at binding energy of 532.3 eV[11b] is observed for both electrodes. The absence of the O(1s) peak in the XPS spectrum obtained on the N electrode (spectrum b in Figure 3A) indicates that during the electrochemically partitioned assembly, no detectable MUA molecules replaced the DDT molecules from the DDT monolayer on the N electrode. As the M and N electrodes were prepared on one substrate, they both experienced the same environmental surroundings before XPS measurements. This precludes the possibility that the O(1s) peak at 532.3 eV on the M electrode arises from oxygen contaminants.

Furthermore, the high-resolution XPS spectra at C(1s) region provide more information about the carbon-related surface chemistry on the M and N electrodes (Figure 3B). For the M electrode, besides the characteristic C(1s) peak at 284.7 eV that arises from the aliphatic hydrocarbon chains, a small peak is observed at higher binding energy, as shown in spectrum a in Figure 3B. This XPS feature can also be obtained on the MUA SAM coated gold electrode prepared by self-assembly in the MUA solution for 12 h (spectrum c in Figure 3B). The shift in binding energy, from the methylene peak, agrees well with the results previously reported.[11b] Therefore, the small discrete peak, arising from the carbon atoms in the carboxylic acid groups, is indicative of the presence of the MUA monolayer on the M electrode. On the other hand, the spectrum on the N electrode after modification step 3 exhibits only a single sharp C(1s) peak, as shown in spectrum b in Figure 3B. On the basis of the above XPS results, it can be concluded that, by using the electrochemically partitioned assembly strategy, MUA and DDT monolayers were successfully prepared on M and N electrodes, respectively.

Location-Selective Assembly of Gold Nanoparticles. Since it has been demonstrated that gold nanoparticles were good building blocks to prepare nanoparticle assemblies,[14b,c,21] the gold colloids were used to produce nanoparticle assemblies in this work. The isoelectric point of the gold colloids prepared by the aqueous reduction of $HAuCl_4$ by sodium citrate at reflux is about 2.[22] As a result, the gold nanoparticles are negatively charged due to the adsorption of anions when the pH > 2. Amino-terminated SAMs are dominantly positively charged in

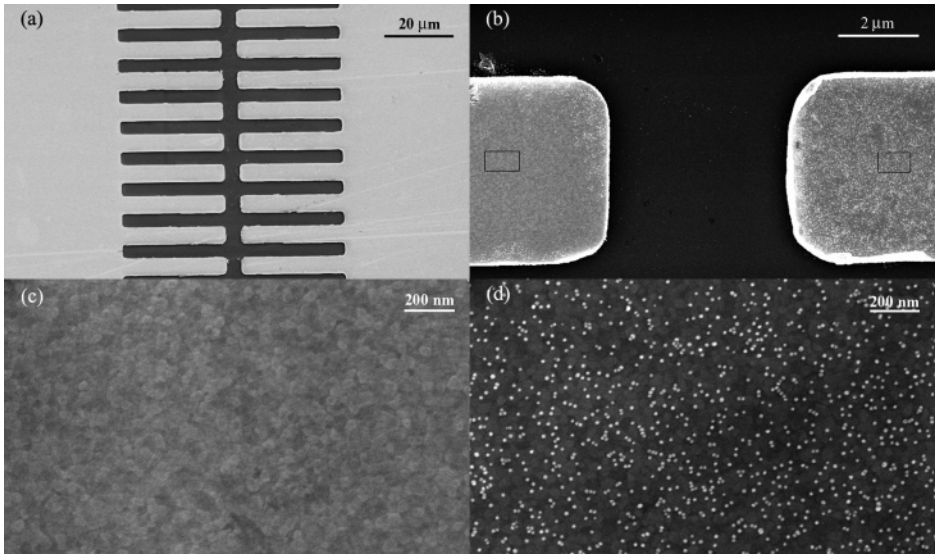

Figure 4. SEM images of (a) gold substrate with two sets of closely spaced microelectrode arrays and (b) ends of two closely spaced microelectrodes after location-selective assembly of gold nanoparticles; (left) the DDT monolayer coated electrode, (right) the p-ATP monolayer coated electrode. High-magnification SEM images of (c) the DDT modified region (the left square shown in b) and (d) the *p*-ATP-modified region (the right square shown in b) after assembly of gold nanoparticles.

the pH range of 3−6, because of the protonation of amino groups,[23] and are usually employed as bridge layers to immobilize gold nanoparticles by the strong electrostatic interactions.[24]

The electrochemically partitioned assembly strategy similar to the one represented in Scheme 1 was employed to prepare the methyl-terminated DDT and the amino-terminated *p*-ATP monolayers on different substrate regions. The resulting samples were characterized by XPS. A N(1s) peak, which arises from the amino groups of *p*-ATP molecules, can be clearly observed at binding energy 399.3 eV in the XPS spectrum obtained in the substrate region coated with the *p*-ATP SAM. The binding energy of N(1s) is in good accordance with the reported values of 399.1 eV for the *p*-ATP monolayer.[15b] For the DDT monolayer coated region, no N(1s) peak appears at the same binding energy position, indicating that the DDT and the *p*-ATP SAMs are successfully deposited on different substrate regions. This result also implies that the electrochemically partitioned assembly technique provides an effective tool to selectively prepare SAMs terminated by different functional groups on particular features of a preexisting pattern at a solid surface.

To clearly demonstrate the location-selective assembly of gold nanoparticles, special substrates prefabricated with two sets of closely spaced (4-μm separation) gold microelectrode arrays were used, as shown in Figure 4a. According to the partitioned-assembly method discussed above, the left and the right electrode arrays were modified with the DDT and the *p*-ATP monolayers, respectively. After modification, the entire substrate was immersed in the gold colloid whose pH was adjusted to 4.5 to allow the adsorption of gold nanoparticles. Figure 4b−d shows results of the location-selective assembly of gold nanoparticles. In the gold colloids with pH 4.5, the nanoparticles are negatively charged due to the adsorption of anions, and the *p*-ATP monolayer is positively charged due to the protonation of amino groups.[23,24] The strong electrostatic interaction between them leads to the immobilization of large numbers of gold nanoparticles on the *p*-ATP-modified electrode, as can be seen in Figure 4b,d. As to the DDT-coated region, since there is no strong interaction between the gold nanoparticles and the uncharged methyl-terminated monolayer,[14b,c] most of the nanoparticles physically adsorbed in this region were removed during the sonication and rinsing procedure. Consequently, only a very small number of nanoparticles are seen in the left electrode (Figure 4b). We believe that these remnant nanoparticles might be anchored to the DDT-modified electrode by physical adsorption or by electrostatic interaction with a very small amount of *p*-ATP molecules that are tangled in the DDT SAM during the immersion in *p*-ATP solution.

Figure 4c,d shows the SEM images of the DDT- and the *p*-ATP-coated region at a higher magnification. They demonstrate a striking contrast in the nanoparticle density. The great difference indicates that the electrode system composed of two sets of closely spaced microelectrode arrays, which were separately modified with DDT and *p*-ATP monolayers, has good location selectivity for the adsorption of gold nanoparticles.

4. Conclusion

We have reported a novel and versatile strategy for the fabrication of partitionally assembled organosulfur monolayers on two different gold electrodes, which are integrated on one substrate and closely spaced to each other, through the use of potential-assisted desorption and adsorption techniques. By using CV and XPS methods, we have demonstrated that the electrochemically partitioned assembly strategy is successful to form different organosulfur monolayers with various functional groups on different regions of the substrate. We also show that the closely spaced gold electrodes, which are insulated from each other and coated with different SAMs, exhibit terminal-group-dependent CV behavior. We believe this SAM-dependent electrochemical behavior arises from the different interactions between the terminal groups on SAMs and the redox couples in solution. Furthermore, on the basis of the electrochemically partitioned assembly approach, we have successfully prepared the location-selective nanoparticle assemblies. The ability of fabricating surface-bound SAMs and nanoparticle assemblies in a controlled manner is very important for many applications; for example, for nanoscaled constructions, it is believed that the electrochemically partitioned assembly method developed in this paper opens an avenue to controllable constructions of high-quality molecular layers and nanostructures on different surface microarchitectures that are closely integrated on one substrate but insulated from each other.

Acknowledgment. Financial support from the National Natural Science Foundation of China (NSFC, 20373005) is gratefully acknowledged.

References and Notes

(1) (a) Ulman, A. *Chem. Rev.* **1996**, *96*, 1533. (b) Love, J. C.; Estroff, L. A.; Kriebel, J. K.; Nuzzo, R. G.; Whitesides, G. M. *Chem. Rev.* **2005**, *105*, 1103.

(2) (a) Chidsey, C. E. D. *Science* **1991**, *251*, 919. (b) Becka, A. M.; Miller, C. J. *J. Phys. Chem.* **1992**, 96, 2657. (c) Finklea, H. O.; Hanshew, D. D. *J. Am. Chem. Soc.* **1992**, *114*, 3173.

(3) (a) Abbott, N. L.; Gorman, C. B.; Whitesides, G. M. *Langmuir* **1995**, *11*, 16. (b) Lahann, J.; Mitragotri, S.; Tran, T.-N.; Kaido, H.; Sundaram, J.; Choi, I. S.; Hoffer, S.; Somorjai, G. A.; Langer, R. *Scinece* **2003**, *299*, 371.

(4) (a) Rubenstain, I.; Steinberg, S.; Yitzhak, T.; Shanzar, A.; Sagiv, J. *Nature* **1988**, *332*, 426. (b) Flink, S.; Boukamp, B. A.; van den Berg, A.; van Veggel, F. C. J. M.; Reinhoudt, D. N. *J. Am. Chem. Soc.* **1998**, *120*, 4652. (c) Wang, Y.; Kaifer, A. E. *J. Phys. Chem. B* **1998**, *102*, 9922.

(5) (a) Colvin, V. L.; Goldstein, A. N.; Alivisatos, A. P. *J. Am. Chem. Soc.* **1992**, *114*, 5221. (b) Diao, P.; Liu, Z. F.; Wu, B.; Nan, X. L.; Zhang, J.; Wei, Z. *ChemPhysChem* **2002**, *3*, 898. (c) Diao, P.; Liu, Z. F. *J. Phys. Chem. B* **2005**, *109*, 20906.

(6) (a) Kumar, A.; Whitesides, G. M. *Appt. Phys. Lett.* **1993**, *63*, 2002. (b) Yan, L.; Zhao, X.-M.; Whitesides, G. M. *J. Am. Chem. Soc.* **1998**, *120*, 6179. (c) Xia, Y.; Whitesides, G. M. *Angew. Chem. Int. Ed.* **1998**, *37*, 550. (d) Hidber, P. C.; Helbig, W.; Kim, E.; Whitesides, G. M. *Langmuir* **1996**, *12*, 1375. (e) Tien, J.; Terfort, A.; Whitesides, G. M. *Langmuir* **1997**, *13*, 5349. (f) Qin, D.; Xia, Y.; Xu, B.; Yang, H.; Zhu, C.; Whitesides, G. M. *Adv. Mater.* **1999**, *11*, 1433.

(7) (a) Widrig, C. A.; Chung, C.; Porter, M. D. *J . Electroanal. Chem.* **1991**, *310*, 335. (b) Walczak, M. M.; Popenoe, D. D.; Deinhammer, R. S.; Lamp, B. D.; Chung, C.; Porter, M. D. *Langmuir* **1991**, *7*, 2687. (c) Shepherd, J. L.; Kell, A.; Chung, E.; Sinclar, C. W.; Workentin, M. S.; Bizzotto, D. *J. Am. Chem. Soc.* **2004**, 126, 8329. (d) Weisshaar, D. E.; Lamp, B. D.; Porter, M. D. *J . Am. Chem. Soc.* **1992**, *114*, 5860. (e) Ron, H.; Rubinstein, I. *J. Am. Chem. Soc.* **1998**, *120*, 13444. (f) Brett, C. M. A.; Kresak, S.; Hianik, T.; Brett, A. M. O. *Electroanalysis* **2003**, *15*, 557.

(8) (a) Imabayashi, S.; Hobara, D.; Kakiuchi, T. *Langmuir* **1997**, *13*, 4502. (b) Hobara, D.; Sasaki, T.; Imabayashi, S.; Kakiuchi, T. *Langmuir* **1999**, *15*, 5073. (c) Mullen, T. J.; Dameron, A. A.; Weiss, P. S. *J. Phys. Chem. B* **2006**, *110*, 14410.

(9) (a) Hsueh, C. C.; Lee, M. T.; Freund, M. S.; Ferguson, G. S. *Angew. Chem. Int. Ed.* **2000**, *39*, 1228. (b) Tender, L. M.; Worley, R. L.; Fan, H.; Lopez, G. P. *Langmuir* **1996**, *12*, 5515.

(10) (a) Tamada, K.; Hara, M.; Sasabe, H.; Knoll, W. *Langmuir* **1997**, *13*, 1558. (b) Chen, S. F.; Li, L. Y.; Boozer, C. L.; Jiang, S. Y. *Langmuir* **2000**, *16*, 9287. (c) Stranick, S. J.; Parikh, A. N.; Tao, Y. T.; Allara, D. L.; Weiss P. S. *J. Phys. Chem.* **1994**, *98*, 7636. (d) Lewis, P. A.; Smith, R. K.; Kelly, K. F.; Bumm, L. A.; Reed, S. M.; Clegg, R. S.; Gunderson, J. D.; Hutchison, J. E.; Weiss, P. S. *J. Phys. Chem. B* **2001**, *105*, 10630. (e) Hobara, D.; Ota, M.; Imabayashi, S. Niki, K.; Kakiuchi, T. *J. Electroanal. Chem.* **1998**, *444*, 113. (f) Hobara, D.; Kakiuchi, T. *Electrochem. Commun.* **2001**, *3*, 154. (g) Phong, P. H.; Ooi, Y.; Hobara, D.; Nishi, N.; Yamamoto, M.; Kakiuchi, T. *Langmuir* **2005**, *21*, 10581.

(11) (a) Xu, S.; Cruchon-Dupeyrat, S. J. N.; Garno, J. C.; Liu, G.-Y.; Jennings, G. K.; Yong, T.-H.; Laibinis, P. E. *J. Chem. Phys.* **1998**, *108*, 5002. (b) Bain, C. D.; Troughton, E. B.; Tao, Y.-T.; Evall, J.; Whitesides, G. M.; Nuzzo, R. G. *J. Am. Chem. Soc.* **1989**, *111*, 321. (c) Diao, P.; Guo, M.; Tong, R. T. *J. Electroanal. Chem.* **2001**, *495*, 98.

(12) Bae, S.-S.; Lim, D. K.; Park, J.-I.; Lee, W.-R.; Cheon, J.; Kim, S. *J. Phys. Chem. B* **2004**, *108*, 2575.

(13) (a) Gooding, J. J.; Wibowo, R.; Liu, J.; Yang, W.; Losic, D.; Orbons, S.; Mearns, F. J.; Shapter, J. G.; Hibbert, D. B. *J. Am. Chem. Soc.* **2003**, *125*, 9006. (b) Patolsky, F.; Weizmann, Y.; Willner, I. *Angew. Chem. Int. Ed.* **2004**, *43*, 2113. (c) Sheeney-Haj-Ichia, L.; Basner, B.; Willner, I. *Angew. Chem. Int. Ed.* **2005**, *44*, 78.

(14) (a) Sugimura, H.; Nakagiri, N. *J. Am. Chem. Soc.* **1997**, *119*, 9226. (b) Li, Q. G.; Zheng, J. W.; Liu, Z. F. *Langmuir* **2003**, *19*, 166. (c) Ling, X.; Zhu, X.; Zhang, J.; Zhu, T.; Liu, M. H.; Tong, L. M.; Liu, Z. F. *J. Phys. Chem. B* **2005**, *109*, 2657.

(15) (a) Hayes, W. A.; Shannon, C. *Langmuir* **1996**, *12*, 3688. (b) Lukkari, J.; Kleemola, K.; Meretoja, M.; Ollonqvist, T.; Kankare, J. *Langmuir* **1998**, *14*, 1705.

(16) Frens, G. *Nat. Phys. Sci.* **1973**, *241*, 20.

(17) (a) Takehara, K.; Takemura, H.; Ide, Y. *Electrochim. Acta* **1994**, *39*, 817. (b) Ma, F.; Lennox, R. B. *Langmuir* **2000**, *16*, 6188.

(18) (a) Porter, M. D.; Bright, T. B.; Allara, D. L.; Chidsey, C. E. D. *J. Am. Chem. Soc.* **1987**, *109*, 3559. (b) Diao, P.; Jiang, D. L.; Cui, X. L.; Gu, D. P.; Tong, R. T.; Zhong, B. *J. Electroanal. Chem.* **1999**, *464*, 61.

(19) (a) Schlenoff, J. B.; Li, M.; Ly, H. *J. Am. Chem. Soc.* **1995**, *117*, 12528. (b) Chidsey, C. E. D.; Bertozzi, C. R.; Putvinski, T. M.; Mujsce A. M. *J. Am. Chem. Soc.* **1990**, *112*, 4301. (c) Biebuyck, H. A.; Bain, C. D.; Whitesides, G. M. *Langmuir* **1994**, *10*, 1825.

(20) (a) Gennett, T.; Weaver, M. J. *Anal. Chem.* **1984**, *56*, 1444. (b) Penner, R. M.; Heben, M. J.; Longin, T. J.; Lewis, N. S. *Science* **1990**, *250*, 1118. (c) Daum, P. H.; Enke, C. G. *Anal. Chem.* **1969**, *41*, 653. (d) Khoshtariya, D. E.; Dolidze, T. D.; Zusman, L. D.; Waldeck, D. H. *J. Phys. Chem. A* **2001**, *105*, 1818.

(21) (a) Freeman, R. G.; Grabar, K. C.; Allison, K. J.; Bright, R. M.; Davis, J. A.; Guthrie, A. P.; Hommer, M. B.; Jackson, M. A.; Smith, P. C.; Walter, D. G.; Natan, M. J. *Science* **1995**, *267*, 1629. (b) Li, H. Y.; Park, S. H.; Reif, J. H.; LaBean, T. H.; Yan, H. *J. Am. Chem. Soc.* **2004**, *126*, 418. (c) Li, Z.; Chung, S.-W.; Nam, J.-M.; Ginger, D. S.; Mirkin, C. A. *Angew. Chem. Int. Ed.* **2003**, *42*, 2306.

(22) Thompson, D.; Collins, I. *J. Colloid Interface Sci.* **1992**, *152*, 197.

(23) (a) Bryant, M. A.; Crooks, R. M. *Langmuir* **1993**, *9*, 385. (b) Andreu, R.; Fawcett, W. R. *J. Phys. Chem.* **1994**, *98*, 12753.

(24) Zhu, T.; Fu, X. Y.; Mu, T.; Wang, J.; Liu, Z. F. *Langmuir* **1999**, *15*, 5197.